Revista Ciencia en Desarrollo. Vol. 16 Num. 1. pp. 182 - 187
enero - junio

DOI: 10.19053/uptc.01217488.v16.n1.2025.16929

Artículo de investigación

Exploration of chemical activation using Mg and Ca chlorides for obtaining biochars from soursop seeds (*Annona muricata*).

Jhoan M. Camargo López[1]✉, Laura M. Esteves[2]✉ y Maria H. Brijaldo[3]✉

[1]Escuela de Ciencias Químicas, Facultad de Ciencias, Universidad Pedagógica y Tecnológica de Colombia UPTC, Avenida Central del Norte, vía Paipa, Tunja, Boyacá, 150003, Colombia
[2]Centro de Química Estrutural, Instituto Superior Técnico, Universidade de Lisboa, Av. Rovisco Pais, Lisboa, 1049-001, Portugal
[3]Escuela de Ciencias Administrativas y Económica, Facultad de Estudios a Distancia, Universidad Pedagógica y Tecnológica de Colombia, Av. Central Norte 39-115 Tunja, 150003, Colombia

Recepción: 1-dic-2023 **Aceptado:** 19-sept-2024 **Publicado:** 20-abril-2025
Cómo citar: Camargo López, J. M., Esteves, L. M., & Brijaldo, M. H. (2025). Exploration of chemical activation using Mg and Ca chlorides for obtaining biochars from soursop seeds *(Annona muricata)*. *Ciencia en Desarrollo*, 16(1). doi: 10.19053/uptc.01217488.v16.n1.2025.16929

Abstract

The capture of CO_2 for subsequent use in the synthesis of high-value-added products using biochars is a solution with significant potential to address environmental issues. However, the results are strongly dependent on the synthesis process and the addition of metal salt that impregnate the carbon surface. To assess the influence of salt on the precursor during pyrolysis, concentrations of 5% and 8% of metallic chlorides ($CaCl_2$ and $MgCl_2$) were employed on pre-cleaned and dried soursop seeds. The objective was to investigate how salt impacts the textural characteristics of the resulting biochars concerning thermal conditions. This process yielded five solids, which were subjected to various characterization techniques.

The results revealed that these solids function as CO_2 adsorbents, with BET surface areas ranging from 140 to 285 m_2/g, as determined by CO_2 analysis. Furthermore, the quantities of adsorbed CO_2 showed variations in the performance of each sample. Additionally, DRIFTS analysis of CO_2 showed sharp peaks corresponding to specific CO_2 adsorptions, particularly in solids activated with $CaCl_2$. The employed characterization techniques facilitated the identification of potential methods to enhance basicity and surface area in solids that exhibited lower performance.

Keywords: environmental crisis, biomass, biochars, chemical activation, environmental remediation.

E-ISSN: 2462-7658

1 Introduction

The utilization of agricultural residues in the Boyacá department has emerged as a viable strategy to mitigate environmental pollution processes and contribute to the sustainable development goals [1]. The effectiveness of lignocellulose pyrolysis significantly impacts the treatments performed, which depend on the added chemical or physical agents to achieve greater volatile matter loss and, consequently, better performance and application of the resulting biochar [2], determining the capacity of biochars to adsorb various contaminants. However, it is crucial to consider that outcomes vary depending on the type of biomass used and the activating agent, taking into account the thermal process. Based on these premises, the activation of new precursors using environmentally benign metal chlorides, such as $CaCl_2$ [3] and $MgCl_2$ [4] has been previously investigated. Nevertheless, a comprehensive comparison between the two approaches has yet to be conducted.

The use of these salts presents an ideal option due to the low concentration required to impregnate precursors and their quality as dehydrating agents, facilitating single-step activation [3]. Furthermore, the electronic deficiency of these metals enables the formation of pores within the range of 2 to 50 nm, which is optimal for the entry of contaminants into the microporous carbon network, where adsorption primarily takes place.

The use of biomass to obtain of biochars for environmental remediation not only provides an effective alternative for contaminant adsorption but also contributes to a circular economy approach based on the carbon cycle. This reduces the need to resort to mineral carbon sources, thereby reducing CO_2 emissions into the atmosphere. In this context, the application of solid adsorbents in CO_2 capture primarily focuses on the preparation and characterization of activated carbon.

The most common precursors for biochar production include African palm shells [5], coconut shells [6], coffee husks [7], Mucuna mutisiana seeds [8], potato and cassava peels [9]. These raw materials are subjected to various preparation conditions, such as the activation method [10], type of activating agent, concentration or rate of activating agent, temperature, and residence times in both carbonization and activation processes.

The soursop seeds Biochar Synthesis method, characterization, and practical applications was designed according to follow Scheme 1:

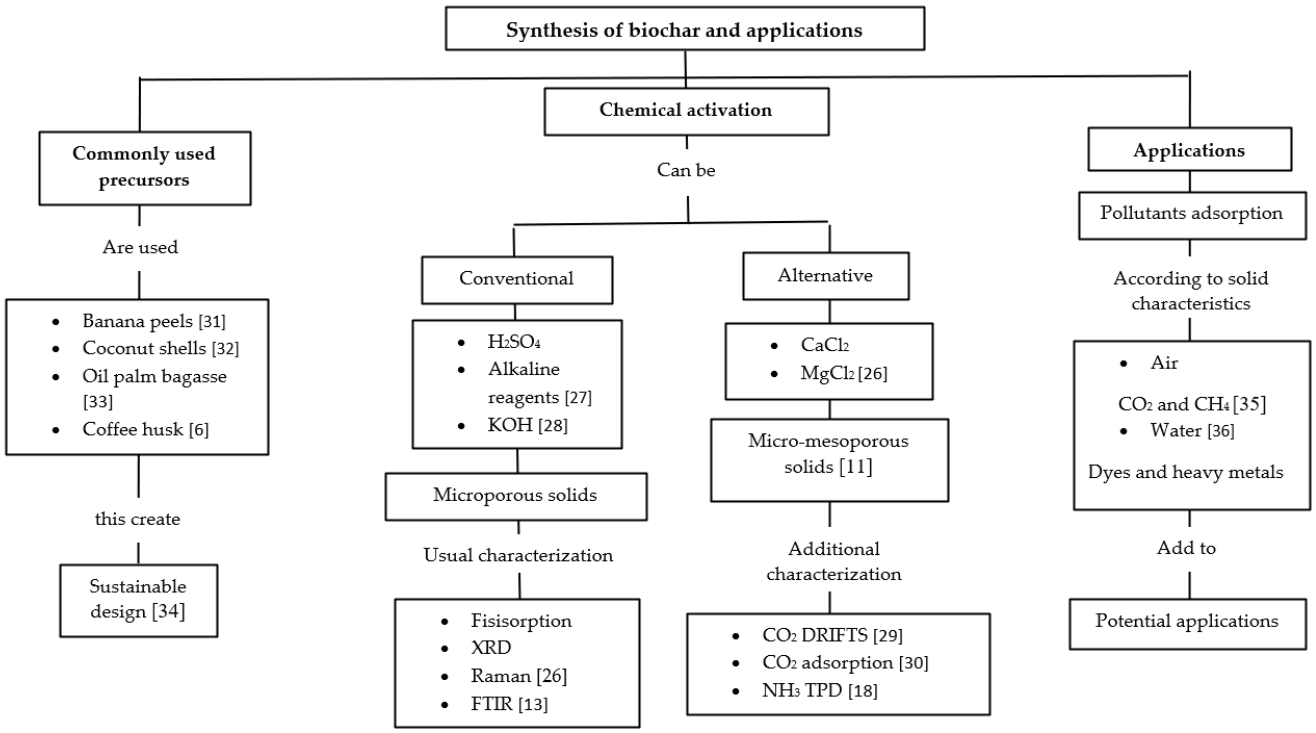

Scheme 1: Synthesis method, characterization, and practical applications of Soursop seeds Biochar.

The use of soursop seeds represents an innovative perspective in the utilization of biomass in the region, while posing the challenge of determining optimal conditions using $CaCl_2$ and $MgCl_2$ to obtain biochars efficient in CO_2 capture, taking into account their chemical and textural characteristics, as well as the effect of the salts on the carbon surface [11]. This is of particular relevance as biomass pyrolysis processes produce bio-oils that may interact with salt oxides, promoting or inhibiting the development of the porous network or chemical surface. In this context, we propose the use of two different concentrations of Mg and Ca metal chlorides for biochar production, comparing their properties through techniques such as FTIR, CO_2 DRIFTS, XRD, CO_2 adsorption, and Raman spectroscopy. This will allow to determine the most suitable activation process and, at the same time, seek improvements in outcomes obtained in processes that yield less favorable results.

2 Materials and methods

The samples were classified according to the activating agent and concentration, as shown in Table 1.

Table 1: samples and abbreviations

Sample	Abbreviation
Soursop seeds	SS
Soursop seeds Biochar	BC
Biochar + $MgCl_2$ 5%	C/Mg5
Biochar + $MgCl_2$ 8%	C/Mg8
Biochar + $CaCl_2$ 5%	C/Ca5
Biochar + $CaCl_2$ 8%	C/Ca8
Heating ramp 1K/min 8%	CaR1

Thermogravimetric analysis was conducted using Setaram 1600 equipment, employing a temperature ramp of 5 K/min up to 1073 K in a nitrogen atmosphere (20 mL/min). Soursop seed samples, pulverized and measured in a 90 μL alumina crucible, exhibited masses of 39.4 mg and 31.2 mg for soursop seed and degreased seeds, respectively [12].

Biochar Preparation

Biochars were produced through pyrolysis with chemical activation of soursop seeds and defatted soursop seeds as precursor materials to obtain biochar (BC). Soursop seeds, obtained from a fruit pulp factory, were washed, dried at 373 K, and crushed to achieve a particle size between 4 and 2 mm. Chemical activation involved a 1:2 ratio mixture of soursop seeds with $CaCl_2$ and $MgCl_2$ as activating agents. The activated solid was then dried for 12 hours at 373 K [5].

The carbons were prepared using a tubular resistor Lindberg Blue M TF55035A-1 at 1073 K for 2 hours, with a flow of 50 mL/min of CO_2 and N_2 mixture. The heating ramp was the same as that used in TGA analysis to retain a certain amount of mass (5 K/min). Activated carbons were treated with HCl 0.01 M to eliminate excess activator and washed with distilled water [13].

Characterization of Carbonaceous Materials The biochars form soursop seed were characterized through of different instrumental techniques. XRD patterns were obtained with a MiniFlex diffractometer, CuKα radiation, and a step increment of 0.05°. Crystal sizes were determined using the FWHM and the Debye-Scherrer equation [14]. Infrared spectra were collected by the FTIR-ATR method using a Thermo Scientific NICOLET iS50 FT-IR spectrometer with a ZnSe ATR cell [15]. CO_2 adsorption spectra were collected using in situ diffuse reflectance with ZnSe windows on the same FTIR equipment [16]. Carbon dioxide adsorption at 293 K was carried out using the Micromeritics ASAP 2020 analyzer to 1 bar [17]. NH_3 desorption was measured using an Auto-ChemII 2920 unit, with He and NH_3 flows at programmed temperatures [18]. Raman spectroscopy measurements were conducted at room temperature using a Witec alpha 300 Confocal Raman microscopy, with an Nd-YAG green laser (532 nm) and 50x objective lens.

3 Results and discussion

Characterization of carbonaceous materials

The infrared spectra of the solids are presented in Figure 1. The resulting spectra exhibit common features in both the biomass and its pyrolysis products. It can be observed that in the solids activated with $CaCl_2$, the bands corresponding to the precursor are better preserved, particularly at lower concentrations. This is clearly manifested by a broad band appearing around 3370 cm^{-1}, which is associated with the vibrations of O-H bonds. Additionally, bands at 1600 cm^{-1} and 1400 cm^{-1} are identified, likely associated with the vibrations of C=O and C=C groups, respectively [19]. These observations indicate a partial decomposition of cellulose compared to samples activated with Mg chlorides. It is worth noting that these bands tend to gradually decrease as the concentration of both activators in the samples increases.

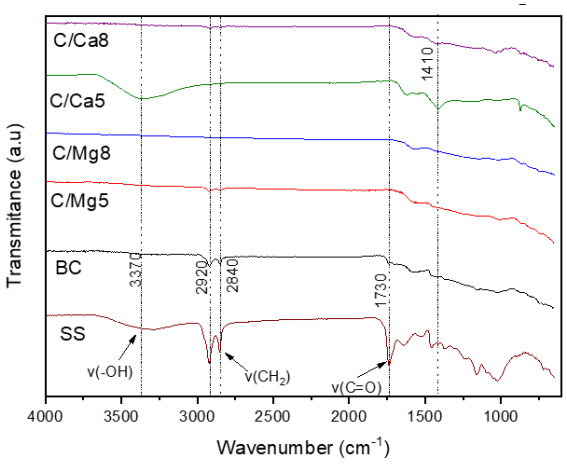

Figure 1: X Ray difraction patterns of biochars. Source: Authors

X-ray diffraction patterns provide evidence of crystallinity presence in the obtained biochar. A characteristic band of graphitic carbon can be observed in the BC, C/Mg5, and C/Mg8 samples in the Figure 2. In the case of solids impregnated with Mg, peaks corresponding to MgO are detected at diffraction angles of 2θ= 43° and 62.5°, and an additional small peak near 37° is noticeable, with its intensity increasing as the concentration of the metallic chloride used in the activation process rises.

Conversely, in the diffractograms of biochars activated with Ca chlorides, there was a decrease in the intensity of peaks indicating the presence of CaO crystals as the concentration increases (2θ= 29.5°) [20]. These X-ray diffraction results clearly reveal the influence of different activators (Mg and Ca) on crystal formation and the structure of the obtained biochars. The peaks at 25° and 43° confirm the formation of crystalline structures of graphitic carbon. The weak diffraction peak at 2θ of 43° is attributed to the a-axis of the graphite structure. Additionally, two signals corresponding to the brucite phase with a cubic structure are identified at 62.30° in 2θ, respectively. The intensity of these signals increases with higher MgO content [21].

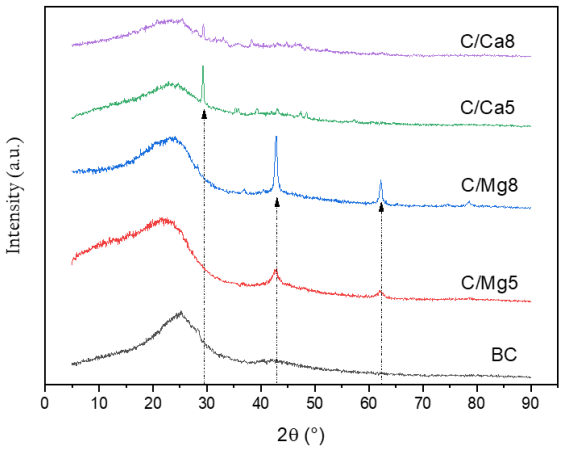

Figure 2: X Ray difraction patterns of biochars. Source: Authors

Surface area measurements were conducted on carbon samples through physical adsorption of carbon dioxide (CO_2) at room temperature, the isotherms of biochars are shown in Figure 3. The results revealed that the adsorbed quantities varied within a range of 20 to 50 cm^3/g, with C/Mg8 carbon displaying the highest adsorption capacity. A significant difference was observed when compared to its activated counterpart with a lower concentration of metallic chloride. Conversely, the carbon activated with calcium chloride

($CaCl^2$) showed no appreciable differences in the values of CO_2 adsorbed when altering the salt concentration. Despite the surface areas being relatively low in comparison to carbons synthesized previously using the same chlorides, as mentioned in Acevedo's study, the amounts of CO_2 adsorbed approached those obtained in such solids, which exceeded 800 m^2/g [22].

Given that CO_2 adsorption is limited to the formation of a monolayer of adsorbate on the solid surface due to strong interactions between gas molecules, it is assumed that the solids predominantly possess a network of narrow pores, accessible only to carbon dioxide molecules. In the case of C/Mg8 carbon, its adsorption isotherm exhibits a slight inflection point, suggesting a modification in the carbon's surface resulting in increased CO_2 adsorption, whether due to a heterogeneous surface or an enhancement in its surface area [23].

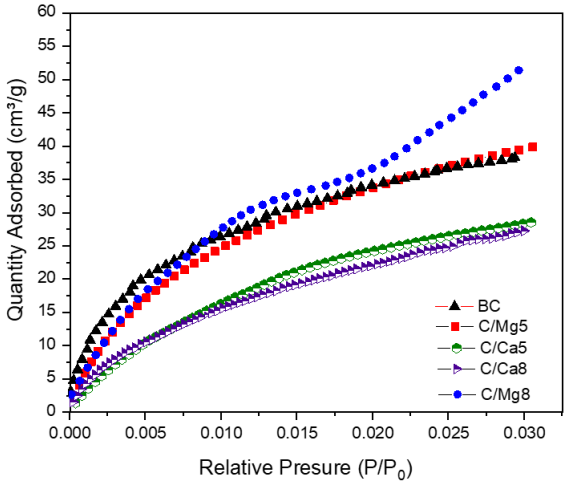

Figure 3: CO_2 Isotherms of biochars

The table 2 summarizes the values of surface area, micropore size, and the amount of adsorbed CO_2 for the synthesized biochars. The carbon with the highest surface area corresponds to the highest concentration of Magnesium Chloride ($MgCl_2$), as well as the solid that showed the best CO_2 adsorption results, whereas, the CaR1 sample showed the lowest surface area, and consequently the CO_2 adsorption capacity was also low.

Table 2: CO_2 adsorption values for biochars

Biochar	S_{BET} area (m^2/g)	Pore size (nm)	Amount of CO_2 adsorbed (cm^3/g)
BC	142	0.5	23
C/Mg5	217	1.1	39
C/Mg8	286	0.6	50
C/Ca5	183	0.8	28
C/Ca8	153	0.8	27
CaR1	140	0.4	23

The CO_2 DRIFT spectra shown in Figure 4 depict several key observations. Firstly, the signals at 2360 cm^{-1} correspond to CO_2 adsorption in the gas phase. Additionally, there are signals near 877 cm^{-1}, 1400 cm^{-1}, and 1580 cm^{-1}, which can be attributed to different vibrational modes of bicarbonates [18]. On the other hand, the signals between 2850 cm^{-1} and 2950 cm^{-1} are indicative of certain hydrogenation species of bicarbonates [14].

From these observations, we can deduce that one of the reasons for the more well-defined bands in the range of 800 cm^{-1} to 1500 cm^{-1} in C/Ca5 is the presence of CaO on the surface of the biochar. This CaO contributes to pore blockage within the solid material's porous network.

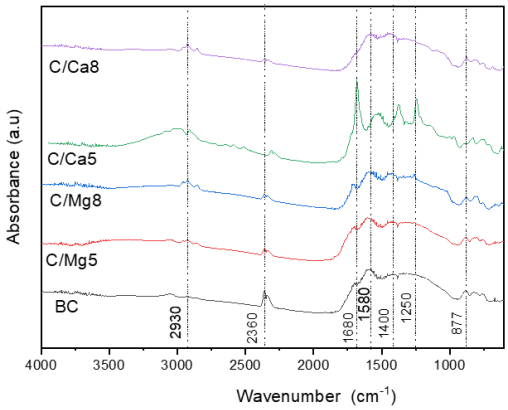

Figure 4: CO_2 DRIFT spectra of biochars

Given that the majority of the precursor's bands, analyzed through FTIR-ATR, are retained in the samples activated with $CaCl_2$, which exhibit lower CO_2 adsorption, it is presumed that volatile matter obstructs the pores and hinders the development of the microporous network. However, a singular sample was subjected to a slower heating ramp (CaR1) using a heatig of 1K/min to verify the formation of graphitic carbon in the specimen through Raman spectroscopy.

The Raman spectra, depicted in Figure 5, reveal distinct bands around 1390 and 1592 cm^{-1}, referred to as the D and G bands, respectively. The G band is linked to a solitary graphite crystal or the E2g mode of hybridization in activated carbon materials [24], whereas the D band signifies polycrystalline graphite [25] or graphite domains featuring structural disorder, indicating flaws in the crystalline structure. As illustrated in Figure 5, there is an increase in the intensity of the D band. Notably, this enhancement is evident through the modification of the heating ramp, rather than through the use of the activating agent.

The Raman spectra of biochars activated with 5% and 8% $MgCl_2$ exhibited prominent bands around 1390 and 1592 cm^{-1}, corresponding to the D and G bands, respectively. These bands are observed more significantly compared to those in biochars activated with $CaCl_2$, where the intensity of the D and G bands is notably lower. However, the CaR1 sample, which was subjected to a slower heating ramp, shows greater intensity in both the D and G bands compared to all other samples, indicating a higher presence of graphitic carbon in this specific sample.

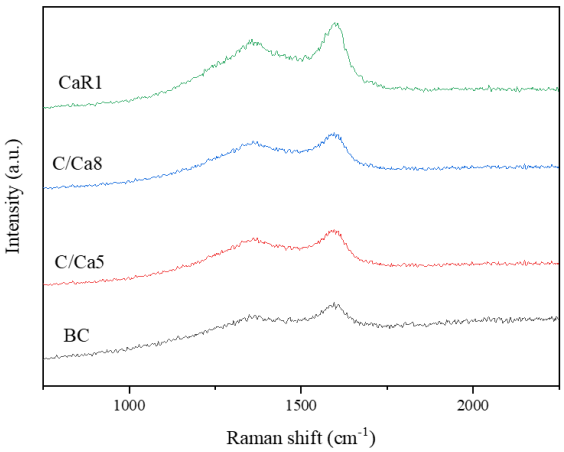

Figure 5: Raman spectra of Ca biochars

Conclusions

The formation of carbonates is observed due to the presence of metal oxides in the biochar, rather than the adsorption of CO^2 in the gas phase. Whereas, the activation using $CaCl^2$ unfavorable since during pyrolysis, calcium remains adhered to the surface of the biochar and the bio-oil from the precursor in the form of CaO. The utilization of $MgCl_2$ increases both the surface area and pore size, which is reflected in the amount of CO^2 adsorbed under normal conditions. However, the presence of MgO on the solid's surface is evidenced by the formation of crystals that grow in size with increasing concentration.

IR bands from the precursor persist more significantly in the solids activated with $CaCl^2$, including bands attributed to -OH and C=O vibrations. This indicates the presence of organic residues, such as fats, from the pyrolysis process on the carbon surface. These residues hinder proper pore formation in the biochar derived from soursop seeds. Thus, the results suggest that activation with $MgCl_2$ demonstrates more promising potential in terms of enhancing CO^2 adsorption capacity and improving the textural properties of the biochar compared to $CaCl^2$. However, addressing the presence of MgO on the solid's surface is essential, as it represents a potential challenge that may affect the efficiency of the adsorption process.

Acknowledgments

The authors greatly acknowledge the support provided by the Universidad Pedagógica y Tecnológica de Colombia, the Grupo de Investigación Catálisis de la Universidad Pedagógica Tecnológica de Colombia GC-UPTC, Grupo de Investigación en Farmacia y Medio Ambiente FARQUIMA and the Vicerrectoria de Investigación y Extensión (VIE) of UPTC by the financial support of Projetc SGI 3567. Special thanks to the institutions and researchers who participated in this research - Escuela de Ciencias Básicas, Universidad Nacional Abierta y a Distancia, Departamento de Química, Facultad de Ciencias, Universidad Nacional de Colombia and Peslac®.

Author contributions

Jhoan M. Camargo Lopez: responsible for the conceptual design of the study and the drafting of the original manuscript. He conducted the comprehensive literature review, designed and performed the experimental procedures, generated and curated the research metadata, and carried out the chemical data analysis. Laura M. Esteves contributed to the validation and interpretation of experimental results and was actively involved in the critical revision and final editing of the manuscript. Maria H. Brijaldo Ramirez also contributed to the validation and interpretation of the data and collaborated in the comprehensive review and refinement of the final version of the manuscript.

Conflict of interest

The authors declare no conflicts of interest.

References

[1] M. A. Yahya, Z. Al-Qodah, and C. W. Z. Ngah, "Agricultural bio-waste materials as potential sustainable precursors used for activated carbon production: A review," *Renew. Sustain. Energy Rev.*, vol. 46, pp. 218–235, 2015, doi: 10.1016/j.rser.2015.02.051.

[2] M. do C. Rangel, F. M. Mayer, M. da S. Carvalho, G. Saboia, and A. M. de Andrade, "Selecting Catalysts for Pyrolysis of Lignocellulosic Biomass," *Biomass*, vol. 3, no. 1, pp. 31–63, 2023, doi: 10.3390/biomass3010003.

[3] D. P. Vargas, L. Giraldo, and J. C. Moreno-Piraján, "CO_2 adsorption on activated carbon honeycomb-monoliths: A comparison of Langmuir and Tóth models,"*Int. J. Mol. Sci.*, vol. 13, no. 7, pp. 8388–8397, 2012, doi: 10.3390/ijms13078388.

[4] Y. Shi, Sajjadi, Baharak Chen, Wei Yin Egiebor, Nosa O., "Synergistic effect of floatable hydroxyapatite-modified biochar adsorption and low-level $CaCl^2$ leaching on Cd removal from paddy soil," *Sci. Total Environ.*, vol. 807, p. 150872, 2022, doi: https://doi.org/10.1016/j.scitotenv.2021.150872.

[5] S. Acevedo, L. Giraldo, and J. C. Moreno, "Caracterização textural e química de carvões ativados prearados a partir de casca da palmeira africana (Elaeis guineensis) por ativação química com $CaCl^2$ y $MgCl_2$," *Rev. Colomb. Quim.*, vol. 44, no. 3, pp. 18–24, 2015, doi: 10.15446/rev.colomb.quim.v44n3.55606.

[6] B. B. Vera Raza, R. A. Mero Intriago, G. A. Burgos Briones, and R. E. Cevallos Cedeño, "Lignocellulosic waste and activated carbon production method," Minerva, vol. 1, no. Special, pp. 122–130, 2022, doi: 10.47460/minerva.v1ispecial.87.

[7] N. Kiggundu and J. Sittamukyoto, "Pryloysis of Coffee Husks for Biochar Production," *J. Environ. Prot. (Irvine,. Calif).*, vol. 10, no. 12, pp. 1553–1564, 2019, doi: 10.4236/jep.2019.1012092.

[8] J. E. Vargas, L. G. Gutierrez, and J. C. Moreno-Piraján, "Preparation of activated carbons from seeds of Mucuna mutisiana by physical activation with steam," *J. Anal. Appl. Pyrolysis*, vol. 89, no. 2, pp. 307–312, 2010, doi: 10.1016/j.jaap.2010.09.009.

[9] L. A. Alonso-Gómez, D. D. Celis-Carmona, Y. F. Rodríguez-Sánchez, J. R. Castro-Ladino, and J. C. Solarte-Toro, "Biochar production from cassava waste biomass: A techno-economic development approach in the Colombian context," *Bioresour. Technol. Reports*, vol. 26, p. 101872, 2024, doi: https://doi.org/10.1016/j.biteb.2024.101872.

[10] M. Lay, A. Rusli, M. Khalil, Z. Ain, A. Hamid, and R. Khimi, "Converting dead leaf biomass into activated carbon as a potential replacement for carbon black filler in rubber composites," *Compos. Part B*, vol. 201, p. 108366, 2020, doi: 10.1016/j.compositesb.2020.108366.

[11] W. J. Liu, H. Jiang, K. Tian, Y. W. Ding, and H. Q. Yu, "Mesoporous carbon stabilized MgO nanoparticles synthesized by pyrolysis of $MgCl_2$ preloaded waste biomass for highly efficient CO_2 capture," *Environ. Sci. Technol.*, vol. 47, no. 16, pp. 9397–9403, 2013, doi: 10.1021/es401286p.

[12] L. Sanabria, C. Lederhos, M. Quiroga, J. Cubillos, H. Rojas, y J. J. Martinez, "Pt y Pd soportado en carbón activado para la oxidación de 5-hidroximetilfurfural a ácido 2,5-furanodicarboxílico", *inycomp*, vol. 19, n. 2, pp. 36–42, 2017 https://doi.org/10.25100/iyc.v19i2.5291

[13] S. Alberto and A. Corredor, "Preparación y caracterización de carbón activado granular obtenido a partir de cuesco de palma africana (Elaeis Guineensis) para la adsorción de CO_2," Doctoral disertation, UNAL Co. Bogotá D.C. 2014.

[14] L. M. Esteves, M. H. Brijaldo, and F. B. Passos, "Decomposition of acetic acid for hydrogen production over Pd/Al2O3 and Pd/TiO2: Influence of metal precursor," *J. Mol. Catal. A Chem.*, vol. 422, pp. 275–288, 2016, doi: 10.1016/j.molcata.2016.02.001.

[15] C. Castañeda, F. Tzompantzi, R. Gómez, and H. Rojas, "Enhanced photocatalytic degradation of 4-chlorophenol and 2,4-dichlorophenol on in situ phosphated sol-gel TiO2," *J. Chem. Technol. Biotechnol.*, vol. 91, no. 8, pp. 2170–2178, 2016, doi: 10.1002/jctb.4943.

[16] H. A. Rojas., P. L. Viviana., M. H. Brijaldo, S. Mancipe., José J. Martínez., A. Gomez. and D. G. Araiza, "Effect of boron on the surface properties of nickel supported on hydrotalcite-type mixed oxides in methanol decomposition," vol. 498, 2020, doi: 10.1016/j.mcat.2020.111262.

[17] L. Giraldo and J. C. Moreno, "Adsorción de CO_2 en carbón activado con diferente grado de activación," *Afinidad*, vol. 67, no. 548, 2010. URL: https://www.raco.cat/index.php/afinidad/article/view/269277

[18] H. A. Rojas, J. J. Martínez, M. H. Brijaldo, and F. Passos, "Producción de alcohol cinamílico a partir de la hidrogenación selectiva de cinamaldehído usando catalizadores de oro soportados en óxidos metálicos," *Rev. la Acad. Colomb. Ciencias Exactas, Físicas y Nat.*, vol. 43, no. 168, pp. 539–549, 2019, doi: 10.18257/raccefyn.852.

[19] P. Schroeder, B. P. do Nascimento, G. A. Romeiro, M. K. K. Figueiredo, and M. C. da C. Veloso, "Chemical and physical analysis of the liquid fractions from soursop seed cake obtained using slow pyrolysis conditions," *J. Anal. Appl. Pyrolysis*, vol. 124, pp. 161–174, 2017, doi: 10.1016/j.jaap.2017.02.010.

[20] J. M. C. López, J. J. Martínez, M. H. Brijaldo, and S. Acevedo, "CO_2 adsorption in biochars obtained from soursop (Anonna muricata) seeds by chemical activation with metallic salts," *Adsorption*, no. 0123456789, 2024, doi: 10.1007/s10450-024-00528-w.

[21] V. Palermo, Palermo, Valeria, Camargo López, Jhoan M., Brijaldo, María H., Acevedo, Sergio, Mancipe, Sonia, Castillo, Juan Carlos, Rojas, Hugo A., Passos, Fabio B., Romanelli, Gustavo P., Martínez, José J., "Biochar-MgO from Soursop Seeds in the Production of Biofuel Additive Intermediates,"*Chempluschem*, vol. 88, no. 11, 2023, doi: 10.1002/cplu.202300401.

[22] S. Acevedo, L. Giraldo, and J. C. Moreno-Piraján, "Kinetic study of CO_2 adsorption of granular-type activated carbons prepared from palm shells," *Environ. Sci. Pollut. Res.*, pp. 1–10, 2023, doi: 10.1007/s11356-023-26423-5.

[23] B. Petrovic, M. Gorbounov, and S. Masoudi Soltani, "Influence of surface modification on selective CO_2 adsorption: A technical review on mechanisms and methods," *Microporous Mesoporous Mater.*, vol. 312, no. 2020, p. 110751, 2021, doi: 10.1016/j.micromeso.2020.110751.

[24] Morán, J.I., Alvarez, V.A., Cyras, V.P. "Extraction of cellulose and preparation of nanocellulose from sisal fibers". Cellulose 15, 149–159 (2008). https://doi.org/10.1007/s10570-007-9145-9

[25] E. Yagmur, Y. Gokce, S. Tekin, N. I. Semerci, and Z. Aktas, "Characteristics and comparison of activated carbons prepared from oleaster *(Elaeagnus angustifolia L.)* fruit using KOH and ZnCl2," Fuel, vol. 267, no. 2019, p. 117232, 2020, doi: 10.1016/j.fuel.2020.117232.

[26] D. P. Vargas, L. Giraldo, and J. C. Moreno-Piraján, "Accessible area and hydrophobicity of activated carbons obtained from the enthalpy characterization," *Adsorption*, vol. 22, no. 1, pp. 3–11, 2016, doi: 10.1007/s10450-015-9721-5.

[27] R. Azargohar and A. K. Dalai, "Steam and KOH activation of biochar: Experimental and modeling studies," Microporous Mesoporous Mater., vol. 110, no. 2, pp. 413–421, 2008, doi: https://doi.org/10.1016/j.micromeso.2007.06.047.

[28] A. S. Ello, L. K. C. De Souza, A. Trokourey, and M. Jaroniec, "Development of microporous carbons for CO_2 capture by KOH activation of African palm shells," *J. CO_2 Util.*, vol. 2, pp. 35–38, 2013, doi: 10.1016/j.jcou.2013.07.003.

[29] L. Proaño, E. Tello, M. A. Arellano-trevino, S. Wang, R. J. Farrauto, and M. Cobo, "Applied Surface Science In-situ DRIFTS study of two-step CO_2 capture and catalytic methanation over," *Appl. Surf. Sci.*, vol. 479, no. 2018, pp. 25–30, 2019, doi: 10.1016/j.apsusc.2019.01.281.

[30] A. Mukhtar, N. Mellon, S. Saqib, S. P. Lee, and M. A. Bustam, "Extension of BET theory to CO_2 adsorption isotherms for ultra-microporosity of covalent organic polymers," *SN Appl. Sci.*, vol. 2, no. 7, pp. 1–4, 2020, doi: 10.1007/s42452-020-2968-9.

[31] A. Selvarajoo, D. Muhammad, and S. K. Arumugasamy, "An experimental and modelling approach to produce biochar from banana peels through pyrolysis as potential renewable energy resources," *Model. Earth Syst. Environ.*, vol. 6, no. 1, pp. 115–128, 2020, doi: 10.1007/s40808-019-00663-2.

[32] K. Yang, J. Peng, C. Srinivasakannan, L. Zhang, H. Xia, and X. Duan, "Preparation of high surface area activated carbon from coconut shells using microwave heating," *Bioresour. Technol.*, vol. 101, no. 15, pp. 6163–6169, 2010, doi: https://doi.org/10.1016/j.biortech.2010.03.001.

[33] A. C. Lua, "A comparative study of the pore characteristics and phenol adsorption performance of activated carbons prepared from oil-palm shell wastes by steam and combined steam-chemical activation," *Green Chem. Eng.*, no. September, 2023, doi: 10.1016/j.gce.2022.11.004.

[34] B. Flores, C. Chacón, and B. Galia, "El desarrollo sostenible y la agenda 21 Sustainable Development, Agenda 21," *Agenda*, vol. 11, no. 2, pp. 164–181, 2009. URL: https://www.redalyc.org/articulo.oa?id=99312517003

[35] F. Rodríguez-Reinoso and J. Silvestre-Albero, Nanoporous Materials for Gas Storage. 2019. DOI: https://doi.org/10.1007/978-981-13-3504-4_8

[36] B. Sajjadi, W. Y. Chen, and N. O. Egiebor, "A comprehensive review on physical activation of biochar for energy and environmental applications," *Rev. Chem. Eng.*, vol. 35, no. 6, pp. 735–776, 2019, doi: 10.1515/revce-2017-0113.